Magnetic excitations in the spinel compound $Li_x[Mn_{1.96}Li_{0.04}]O_4$ ($x=0.2, 0.6, 0.8, 1.0$): How a classical system can mimic quantum critical scaling

Thomas Heitmann,[1] Alexander Schmets,[2,3] John Gaddy,[1,2] Jagat Lamsal,[1,2] Marcus Petrovic,[2] Thomas Vojta,[4] and Wouter Montfrooij[1,2]

[1]*The Missouri Research Reactor, University of Missouri, Columbia, Missouri 65211, USA*

[2]*Department of Physics and Astronomy, University of Missouri, Columbia, Missouri 65211, USA*

[3]*Reactor Institute Delft, Technical University of Delft, 2629 JB Delft, The Netherlands*

[4]*Department of Physics, Missouri University of Science and Technology, Rolla, Missouri 65409, USA*

(Received 7 April 2009; revised manuscript received 7 December 2009; published 14 January 2010)

We present neutron-scattering results on the magnetic excitations in the spinel compounds $Li_x[Mn_{1.96}Li_{0.04}]O_4$ ($x=0.2, 0.6, 0.8, 1.0$). We show that the dominant excitations below $T\sim 70$ K are determined by Mn ions located in clusters, and that these excitations mimic the dynamic scaling found in quantum critical systems that also harbor magnetic clusters, such as $CeRu_{0.5}Fe_{1.5}Ge_2$. We argue that our results for this classical spinel compound suggest that the unusual response at low temperatures as observed in quantum critical systems that have been driven to criticality through substantial chemical doping is (at least) partially the result of the fragmentation of the magnetic lattice into smaller units.

DOI: 10.1103/PhysRevB.81.014411 PACS number(s): 64.70.Tg, 64.60.ah, 75.50.Lk

I. INTRODUCTION

Metals that harbor magnetic ions can exhibit long-range magnetic order.[1,2] The interaction mechanism responsible for this ordering is the Ruderman, Kittel, Kasuya, Yosida interaction;[3–6] this mechanism describes how conduction electrons get polarized by atomic magnetic moments, and how they in turn can line up neighboring moments. The strength of the interaction depends both on the degree of overlap between the localized electronic states and the extended conduction-electron states, as well as on the distance between the neighboring moments. Since the interaction is mediated by the conduction electrons, the ensuing pattern of magnetic ordering reflects the shape of the Fermi surface rather than the crystal lattice, resulting in incommensurate ordering.

By compressing the crystal lattice, the degree of hybridization between the localized and extended states can be tweaked,[7] resulting in a change to the magnetic-ordering tendencies. In fact, if the hybridization becomes very strong, the conduction electrons shield the magnetic moments via the Kondo mechanism. This results in a nonmagnetic metal[7] where conduction electrons and magnetic moments have combined to form heavy quasiparticles.[8,9] This heavy-fermion state is reflected in the macroscopic properties[9] such as the specific heat of the metal.

By applying just the right amount of lattice compression (or expansion), the metal can be tweaked to such an extent that the system will be on the verge of magnetic ordering at $T=0$ K,[7–9] while the magnetic moments are completely[10,11] [see Fig. 1(a)], or almost completely[12] [Fig. 1(b)] shielded. The metal is said to be at the quantum critical point (QCP), and its macroscopic properties (specific heat, resistivity, and susceptibility) are no longer described by Fermi-liquid theory. This non-Fermi-liquid (nFl) state of matter[8,9] can also be accompanied by dynamic scaling laws.[13] For instance, when the system is probed on a microscopic scale such as in neutron-scattering experiments, its response to a perturbation from equilibrium by an amount of energy E while at a temperature T, depends only on the ratio E/T.[12–16]

The emergence of E/T scaling was particularly surprising since it occurred not only in systems that were (most likely) just below[17] the upper critical dimension[8] [$CeCu_{5.9}Au_{0.1}$ (Ref. 12)] but also in systems that were manifestly above the upper critical dimension [$UCu_{5-x}Pd_x$ for $x=1.0$, 1.5 (Refs. 13 and 14) and $Ce(Ru_{0.24}Fe_{0.76})_2Ge_2$ (Ref. 15)]. Montfrooij *et al.*[18] suggested a way out of this apparent contradiction based on the disorder present in a system[19] when it is driven to the QCP by means of chemical substitution. Their arguments are summarized in Fig. 1(c). The same isovalent substitution that provides chemical pressure in $Ce(Ru_{0.24}Fe_{0.76})_2Ge_2$ also introduces local changes in the interatomic distances on the order of 0.05 Å. Though small, these changes are sufficient to affect the orbital overlap between adjacent atoms such that a distribution of Kondo shielding temperatures is effectively introduced. Consequently, upon cooling, the Ce moments in the vicinity of Ru substitutions will become shielded at different temperatures than those away from Ru substitutions. This leads to a percolation network following the random distribution of Ru dopant positions. This region is somewhat similar to a quantum Griffiths region,[19–21] but the microscopic physics is more complex because it also involves Kondo disorder.[22]

Note that the emergence of such a percolation network is unavoidable since in a system that is on the verge of ordering any change, no matter how small, will make a significant difference. This was shown in the heavy-fermion compound $Ce(Ru_{0.24}Fe_{0.76})_2Ge_2$.[18] Starting from the heavy-fermion system $CeFe_2Ge_2$,[23] upon *increased* doping x of Ru on the Fe sites $Ce(Ru_{0.24}Fe_{0.76})_2Ge_2$ orders magnetically at 0 K once 1:4 Fe ions have been substituted.[15,24] This isovalent substitution takes place on sites that are not nearest neighbors to the moment carrying Ce sites. Thus, one could have expected the effects of this chemical doping to be uniformly spread out over the crystal lattice. However, instead of observing that all the magnetic moments evolve with temperature along

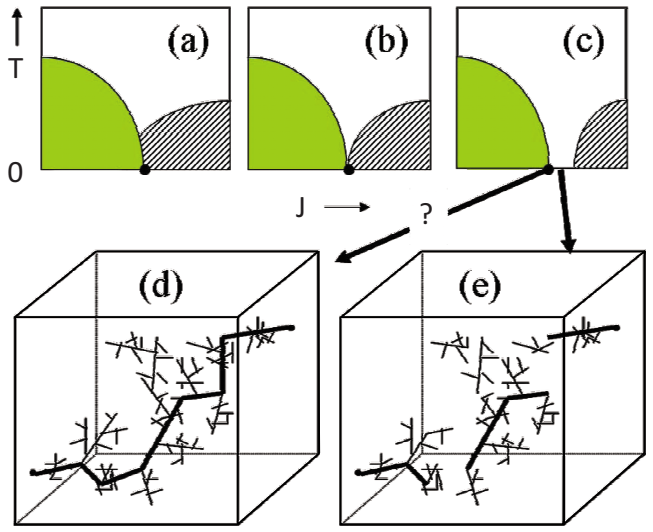

FIG. 1. (Color online) Figure reproduced from Ref. 18. The magnetic phase diagram in the vicinity of a QCP (black dot) as a function of the coupling strength J between local moments and the electron spins. This coupling strength can be tweaked by applying hydrostatic or chemical pressure. The striped areas indicate that the moments are fully shielded, the solid areas are the region where long-range order is present. (a) The Hertz-Millis scenario (Refs. 10 and 11) where ordering is established through a spin-density wave instability of the Fermi surface. (b) The local moment scenario (Refs. 12 and 17) where the QCP is the point where moments can first survive, with decreasing J, all the way down to 0 K. (c) Local variations in interatomic distances have resulted in a spread in shielding temperatures yielding a region of the phase diagram between where moments are completely shielded and where the (partially shielded) moments order (Ref. 18). In this region the surviving (down to 0 K) moments are located in clusters that are not interconnected, as shown in part (e). In this latter scenario, the QCP would correspond to the presence of a lattice spanning cluster, as depicted in part (d).

the lines sketched out in Fig. 1(a) or 1(b), unambiguous evidence[18] for the emergence of magnetic clusters inherent to a percolation network [Fig. 1(c)] was found.

The emergence of magnetic clusters in QCP systems upon cooling should greatly influence the response of these systems and might well explain some of the unusual nFl properties. When a system changes its morphology from a three-dimensional system to some sort of a fractal structure, its response should change accordingly.[25] For example, when a magnetic cluster becomes isolated from the rest of the system, this cluster might well be forced to order magnetically since the thermal energy required to keep this system disordered might no longer be available. After all, the lowest available magnon energy increases with decreasing cluster size because the longest wavelength of such a disordering fluctuation cannot exceed the size of the cluster. Thus, cluster formation would be reflected in the specific heat of the system; whenever a cluster becomes isolated and is forced to order magnetically because of finite-size effects, the loss of entropy will show up in the specific heat, bestowing an unusual temperature dependence upon the specific heat that cannot be described by any theoretical model[10,11,17] that treats the moment shielding as being equivalent on all lattice sites.

The observed E/T scaling[12–15,26] might also be directly or indirectly linked to the formation of magnetic clusters. It could be a direct result because the fractalization of the system could drop the dimensionality of the system to below the upper critical dimension.[8] Or it might be an indirect result since the newly formed (and still forming upon cooling) clusters can now act as superspins that have their orientation controlled by a very small thermally activated barrier $\sim e^{-\Delta/T}$. And, akin to the emergent excitations of such a cluster "protectorate"[27] observed in the spinel compound $ZnCr_2O_4$, the reorientations of these magnetic clusters could well be the local energy modes most relevant to the dynamics near the QCP.

Here we investigate whether E/T scaling might indeed be linked to the formation of magnetic clusters upon cooling. To do so, we study the classical spinel system $Li_x[Mn_{1.96}Li_{0.04}]O_4$ ($x=0.2,0.6,0.8,1.0$) by means of inelastic neutron-scattering experiments. This is an extension of the work of Lamsal *et al.*[28] who investigated the possibility of E/T scaling in the $x=1.0$ compound. We show that the dynamics of the magnetic clusters that are present in these systems[29] below $\sim$70 K do indeed mimic E/T-scaling behavior for all concentrations x; these concentrations cover geometrically frustrated short-range magnetism ($x=1.0$) to long-range magnetic ordering ($x=0.2$). Thus, we show that the behavior previously associated with quantum criticality, which was solely ascribed to the competition between ordering and shielding tendencies, is instead strongly influenced by the emergence of magnetic clusters in these QCP systems.

II. EXPERIMENTS AND RESULTS

A. Brief literature review $LiMn_2O_4$

Stoichiometric $LiMn_2O_4$ undergoes a charge-ordering (CO) transition at 290 K (Refs. 30 and 31) that is accompanied by a transition from a cubic to an orthorhombic structure. The CO structure of the Mn^{3+} and Mn^{4+} B-site ions in the insulating phase has been resolved by Rodriguez-Carvajal *et al.*[31] Upon cooling down further to below 66 K, long-range antiferromagnetic (AF) ordering develops[32] despite the large degree of geometric frustration inherently present in a lattice that has spins located at the vertices of corner-sharing tetrahedra. The low-temperature magnetic structure has not been resolved yet.[32,33]

Upon doping (y) with Li on the Mn sites, $Li_x[Mn_{2-y}Li_y]O_4$ becomes a material that has applications as a component of a light-weight battery.[30] The spinel structure is robust against Li substitution y on the Mn sites while maintaining the capacity for Li removal from the A sites, however, the $\sim$300 K crystallographic phase transition is completely suppressed despite the fact that the CO transition remains. This suppression of the structural transition near room temperature is a boon to the battery industry as it prevents the degradation of the material during recharging cycles of the battery.[30] Neutron-scattering studies[34] and muon investigations[35,36] on the doped material have shown that long-range magnetic order is destroyed for $y>0.02$ and

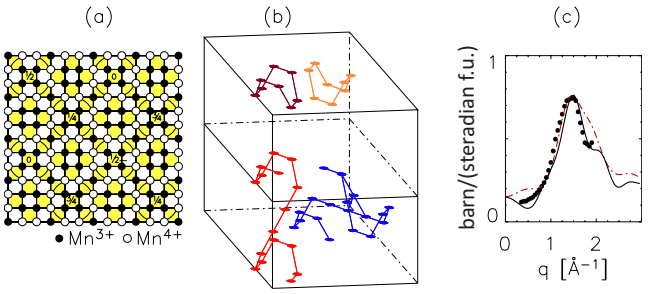

FIG. 2. (Color online) (a) The unit cell for stoichiometric $LiMn_2O_4$ projected along the c axis. The Mn^{4+}-ions (open circles) form isolated eightfold rings, Ref. 31, while the Mn^{3+} ions (filled circles) form columns along the c direction. The numbers within the rings denote their z position in the unit cell (b) Two unit cells stacked along the c axis. Two isolated ring clusters are shown at the top of the figure. Upon Li substitution on the Mn sites (or Mn removal), some Mn^{3+} ions will become Mn^{4+} ions, leading to modified rings (Ref. 29) and linked rings, two possibilities of which are shown in the bottom half of the figure. (c) The observed elastic scattering in $Li[Mn_{1.96}Li_{0.04}]O_4$ at 30 K (Ref. 38) (circles). The two-ring clusters [linked along the c direction; solid line, corresponding to the bottom left cluster in Fig. 2(b) or linked along the ab direction; dashed line, corresponding to the bottom right cluster in Fig. 2(b)] give a satisfactory description (Ref. 29) of the neutron data.

$x>0.3$, and that the material appears to enter a spin glass phase around 15–25 K (with the transition temperature dependent upon the exact Li content[36]). For the compound with $y=0.04$, long-range magnetic order is re-established below ~35 K when the A sites are heavily depleted ($x=0.2$). Note that the long-range ordering pattern found for $x=0.2$ is not the same as the long-range ordering pattern observed[32] in stoichiometric $LiMn_2O_4$ below 66 K, instead it is described by the structure established[37] in λ-Mn_2O_4.

Recently, Gaddy *et al.*[29] have shown that the short-range order observed in $Li_x[Mn_{1.96}Li_{0.04}]O_4$ ($x=1.0$) corresponds to the presence of magnetic clusters of Mn^{4+} ions. Their work was based on the observations by Schimmel *et al.*[38] that the dynamics associated with Mn^{4+} ions are much slower than those of the Mn^{3+} ions; below ~20–25 K (Refs. 35 and 38) the spin dynamics of the Mn^{4+} ions are so slow that the spins appear to be frozen. The Mn^{4+} ions are the ones that couple antiferromagnetically to each other (see Fig. 2), and line up with their immediate neighbors below ~70 K to form the magnetic clusters. These clusters weakly interact with each other, while the overall spin (superspin) of the cluster can reorient itself. The Mn^{3+} ions do not appear to partake in any cluster formation in this $y=0.04$ compound. Gaddy *et al.*[29] found that the backbone of these magnetic clusters [see Fig. 2(a)] are formed by eightfold rings of AF-coupled Mn^{4+} ions (Ref. 31) corresponding to the CO pattern of the stoichiometric compound. We summarize these observations in Fig. 2. The Li substitution on the Mn sites changes some of the Mn^{3+} ions to Mn^{4+} ions, producing links between the eightfold Mn^{4+} clusters[29] [see Fig. 2(b)]. Gaddy *et al.* argued that the clusters shown in Fig. 2(b) only weakly interact with each other and that the low-temperature ($T<70$ K) dynamics of the $x=1.0$ system are dominated by the dynamics of these clusters in the sense that these clusters behave as a collection of weakly interacting superspins. This dominance of the dynamics by clusters is similar to the case of $ZnCr_2O_4$.[27] We will revisit the arguments by Gaddy *et al.* and Lamsal *et al.* in the following after we present and interpret our new neutron-scattering experiments.

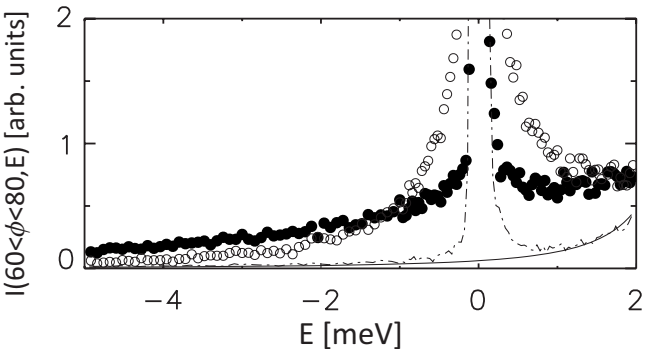

FIG. 3. Details of representative data sets for the new ILL experiments showing the scattering for $x=1.0$ in the window $60° < \phi < 80°$ at 150 K (filled circles) at 41 K (open circles), the empty container scattering (dashed-dotted curve) and the time-independent background (solid line) as obtained from an empty spectrometer run. As can be seen, the container scattering is negligible for $|E| > 0.5$, and the data correction only requires subtraction of the time-independent background for $|E| > 0.5$, the range we used to test dynamic scaling laws.

B. Experimental setup and data reduction

We have performed neutron-scattering experiments on $Li_x[Mn_{1.96}Li_{0.04}]O_4$ (with $x=1.0$, 0.8, 0.6, and 0.2) using the IN6 time-of-flight spectrometer at the Institute Laue-Langevin (ILL) and the TRIAX triple-axis spectrometer at the Missouri Research Reactor (MURR). The setup for the ILL experiments was identical to the pilot experiments[38] on $Li[Mn_{1.96}Li_{0.04}]O_4$; the spectrometer was operated using a fixed neutron incident energy of 3.12 meV. The amount of sample for each x was about 1.5 g, and each sample was measured for about 12 h for a series of temperatures between 2 and 320 K. Empty container runs at 50 K showed that most of the container background was restricted to the elastic channels (see Fig. 3), and that the time-independent background was the same as in the pilot experiments. The quasielastic channels, which we use in our search for E/T scaling, were corrected for this time-independent background. Since the amount of sample was very small compared to the pilot experiments where 25 g was used, we did not need to correct the data for any attenuation effects (which were already small for the 25 g pilot experiment).

The TRIAX experiments for the $x=1.0$ composition were undertaken to extend the range of temperatures available for following the evolution of the magnetic scattering for $T<100$ K. For these experiments, 2 g of powder was placed in a slab sample cell which was housed inside a closed cycle refrigerator. The spectrometer was operated at a fixed final energy E_f of 13.7 meV, with sapphire and PG/Si filters in the incoming beam, and PG filters in the scattered beam. Empty

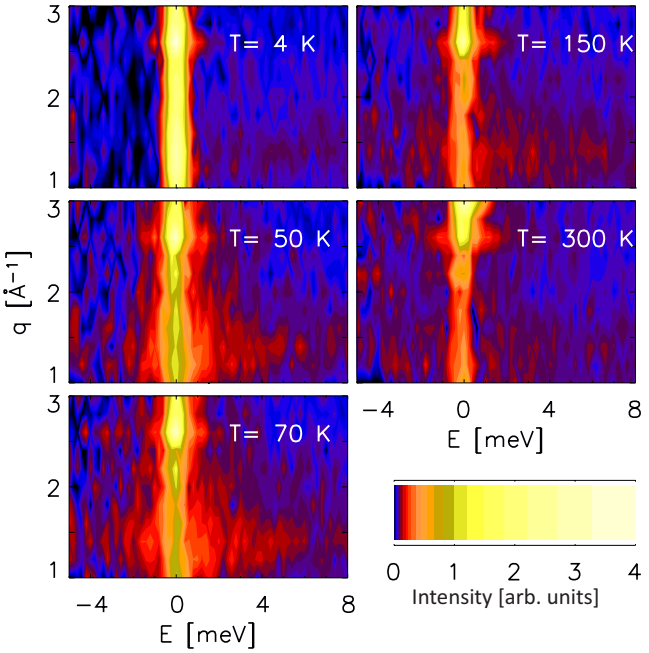

FIG. 4. (Color online) The TRIAX data for $x=1.0$ after background correction for temperatures indicated in the figure. The critical scattering associated with cluster formation around ~70 K (Refs. 29 and 32) shows up as increased intensity in the inelastic channels. Note that this critical scattering extends over a wide range of temperatures, which in turn reflects the frustration (Ref. 27) inherent in systems of this type.

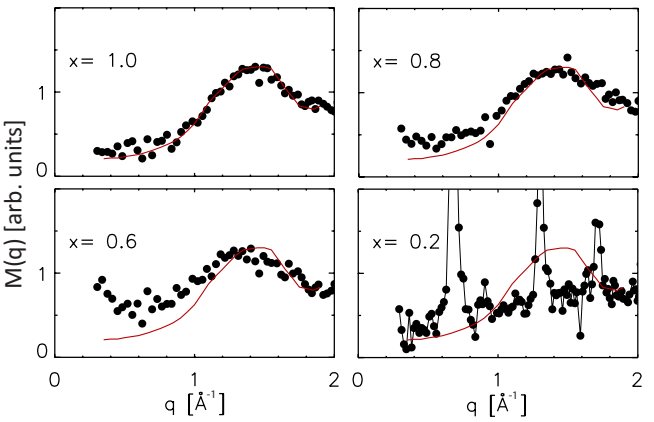

FIG. 5. (Color online) The magnetic form factor (circles) is obtained as the energy integrated scattering, $M(q) = \int_{-0.15\ \mathrm{meV}}^{0.15\ \mathrm{meV}} I(q,E,T=24\ \mathrm{K})dE$, associated with the magnetic clusters for four compositions given in the figure. This scattering, determined from the total magnetic scattering at $T=24$ K in the energy window $|E|<0.15$ meV represents the slowest—or even frozen in—dynamics of the clusters, yielding the magnetic form factor of the clusters. The almost completely lithium depleted sample ($x=0.2$) displays long-range order [sharp Bragg peaks (Ref. 37)], as well as a substantial amount of short-range order. The data have been normalized to sample weight, but an absolute normalization was not possible. For reference, the absolutely normalized data at $x=1.0$ (scaled to give the best agreement with the new ILL data) obtained from the pilot experiment (Ref. 38) are shown by the solid lines in each figure.

sample holder runs taken at the same temperatures as the filled sample holder were used to correct the data for background scattering. The data were also corrected for the monitor contamination resulting from higher order neutrons reaching the monitor. These higher order neutrons are reflected by the incident-beam monochromator and counted by the monitor, but are filtered out by the PG filter in the scattered beam. This results in the monitor counting more neutrons than were actually used in the experiment, however, the correction factor is well known for TRIAX. We show the fully corrected scattering in Fig. 4.

C. Short-range magnetic structure for $T<70$ K

Next, we show that clusters are present for all concentrations x and that these clusters are so weakly interacting with each other that we can treat the clusters as local entities, e.g., we wish to show that we can write the magnetic-scattering intensity $I(q,E,T)$ as the product

$$I(q,E,T) = M(q)f(E,T) \tag{1}$$

with $M(q)$ the form factor of the clusters. Detailed results for the $x=1$ compound[38] show that the dynamics of the Mn^{4+} spins freeze out around ~25 K while the Mn^{3+} spins can still reorient themselves. Following an identical procedure, we plot the frozen in component for all concentrations x in Fig. 5. In order to determine this component of the magnetic scattering, which yields the magnetic form factor $M(q)$ of the clusters, we subtracted the energy integrated scattering $I(\phi,|E|<0.15)$ at $T=100$ K at a given scattering angle ϕ from the intensity measured in the same energy window at $T=24$ K. The latter temperature was chosen to be reasonably close to the glass transition for all concentrations x,[39] yet high enough so that the slowing dynamics of the Mn^{3+} ions would not interfere with the determination of the magnetic form factor of the Mn^{4+} clusters. No further data correction is required for the ILL data sets, and comparison between the new results for $x=1.0$ and the pilot experiments[38] at $x=1.0$ yield identical outcomes (see Fig. 5).

Figure 5 shows that a frozen-in component can easily be determined from the experiments for all x; it is very likely that this frozen-in component only involves the Mn^{4+} ions, however, we cannot entirely rule out that some Mn^{3+} spins are involved as well. The reason for this is that our new data were taken on much smaller amounts of sample with the result that the sample transmissions could not be determined accurately enough in our scattering experiments for us to be able to carry out an absolute normalization required for an unambiguous identification. Notwithstanding, the overall similarity between all concentrations coupled with the fact that both fast and slow dynamics can indeed be observed for all concentrations leads us to infer that the frozen-in component most likely originates in the Mn^{4+} spins. In addition, we have measured the ac susceptibility for all concentrations x.[39] These susceptibility measurements show that phase transitions take place around $T\sim70$ K (which we identify as the cluster-formation temperature) and around $T\sim20$ K (which we identify as the freezing temperature) for all x. Finally, we note that in the remainder of this paper we study the dynam-

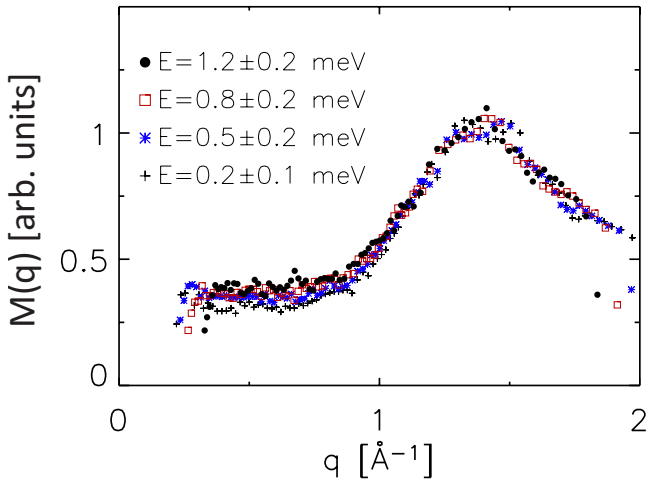

FIG. 6. (Color online) The magnetic form factor $M(q)$ for the $x=1.0$ sample at 50 K as determined from energy integration over the energy transfers shown in the plot. In order to evaluate the shape of the resultant curves, we have normalized each curve to the average intensity in the q range $1.25<q<1.5$ Å^{-1}.

ics of the clusters; whether some Mn^{3+} spins might be part of the clusters (or not) is actually not relevant to our arguments. Bearing this in mind, we shall refer to the clusters in the following as Mn^{4+} clusters.

Figure 5 displays the evolution of the Mn^{4+} clusters upon addition of more Mn^{4+} ions to the lattice. The clusters gradually change from the ones determined for the fully lithiated sample ($x=1.0$) (Ref. 29) to the long-range order visible in the almost fully delithiated sample ($x=0.2$). The positions of the magnetic Bragg peaks seen in the $x=0.2$ sample (Fig. 5) correspond exactly to the magnetic structure resolved for λ-Mn_2O_4 by Greedan *et al.*[37] We have not attempted to resolve the short-range magnetic structure for the intermediate concentrations $x=0.6$ and 0.8. With the addition of more and more Mn^{4+} ions, the number of possibilities for the various cluster shapes becomes too large to try to fit to any particular cluster shape distribution. Instead, we use $M(q)$ as determined from experiment.

D. Length scale independence of the magnetic fluctuations

Having established the presence of a component that freezes out below $T\sim 20-25$ K for all concentrations, we show that the dynamics of this component above the freezing transition exhibits all the characteristics of a collection of weakly interacting clusters. First, the proposed decoupling given in Eq. (1) implies that an energy integration of $I(q,E,T)$ over any energy window for any temperature between where the clusters form and where they freeze out should yield identical shapes proportional to $M(q)$. We show such integrations for the $x=1.0$ compound for $T=50$ K in Fig. 6. The q dependence of the curves shown in this figure is indeed very close to the form factor of the frozen-in component shown in Fig. 5.

Second, when we plot the measured scattered intensity divided by $M(q)$ we should see a collapse of all data onto a single curve [given by $f(E,T)$ in Eq. (1)]. We show this

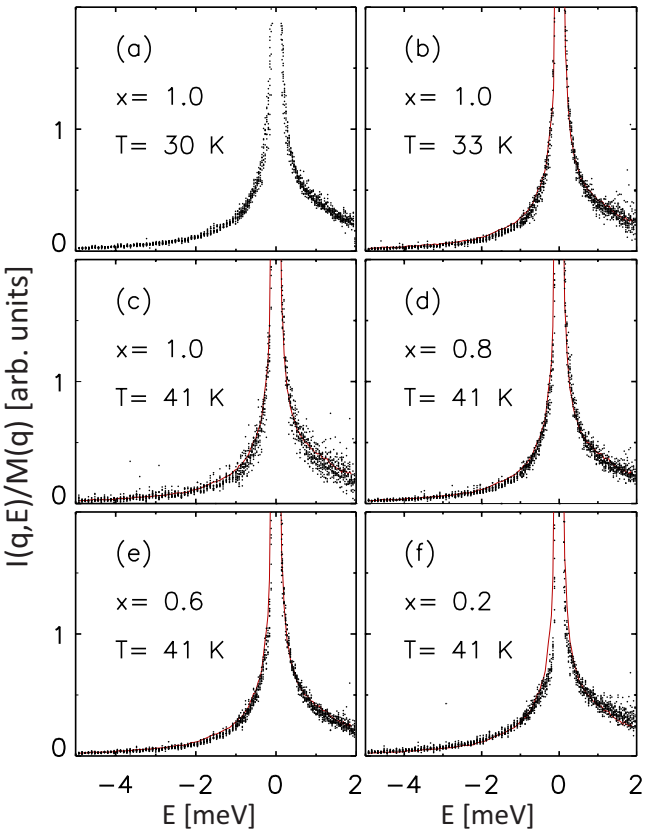

FIG. 7. (Color online) (a) The energy dependence of the scattered intensity $I(q,E)$ for 13 q values $0.5<q<1.8$ Å^{-1} at $T=30$ K for the pilot experiment (Ref. 38). The energy resolution is given by the sharp incoherent nuclear peak. The data have been normalized to the magnetic form factor $M(q)$ of the clusters, which has been determined from $M(q)=I(q,E=0.6$ meV) (see text). All data lie on a single curve, implying that the cluster dynamics are independent of q. (b)–(f) same as part (a), but now for the new ILL data taken at $x=1.0$, 0.8, 0.6, and 0.2, respectively, at $T=33$ K [part (b)] and at $T=41$ K [parts (c) through (f)]. The solid lines in part (b)–(f) are the smoothed data from part (a) to show the consistency between the data sets at $T\sim 30$ K and to provide a reference for $T=41$ K. The scatter of the data points in part (c) is because the particular experimental run was shorter than the ones shown in the other parts of the figure.

replotting of the data in Fig. 7 for all concentrations x. In here, we have used the scattering at $E=0.6$ meV as a measure for the magnetic form factor $M(q)$. Whereas the particular value of E is not important in this procedure (as shown in Fig. 6), picking energy transfers that are away from the elastic channels greatly facilitates the procedure since we do not have to worry whether the data have been corrected for all unwanted elastic scattering effects. The data shown in Fig. 7 do indeed collapse onto the same curve as predicted by Eq. (1), independent of the value of q. Thus, similar to the fully lithiated case,[28] the dynamics for all x do not show any length scale dependence (see Fig. 7), at least in the range $0.5<q=2\pi/\lambda<1.8$ Å^{-1}. Thus, we can safely conclude that clusters are indeed present and that these clusters are weakly interacting. In fact—as was already clear from Fig. 5—even the $x=0.2$ sample shows a large amount of short-range order

that we interpret as being associated with remnant clusters.

III. DISCUSSION

Published data[34,38] together with our present neutron-scattering experiments show that long-range order in $Li_x[Mn_{1.96}Li_{0.04}]O_4$ does not emerge for $x=1.0$, 0.8, and 0.6 down to 2 K, and that substantial amounts of short-range order are still left in the $x=0.2$ compound that does show long-range order below ~33 K. All our results point toward magnetic clusters of Mn^{4+} ions being present for all concentrations and to these clusters dominating the dynamic response. This makes this family of compounds an ideal testbed for investigating whether quantum critical scaling laws[12–15,26] could, in fact, be associated with cluster formation in such systems. After all, $Li_x[Mn_{1.96}Li_{0.04}]O_4$ is a purely classical system (from a phase transition point of view[36]) that is disordered because of geometric frustration and Li/Mn disorder; clusters of AF-aligned Mn^{4+} ions (superspins) are present below ~70 K.[29] The fact that the system's phase transition is classical follows from neutron-scattering results that show the cluster dynamics freezing out ~20–25 K for all values of x, and from susceptibility measurements[39] that show a phase transition around ~20–25 K for all x. Insulating $Li_x[Mn_{1.96}Li_{0.04}]O_4$ should not exhibit any type of quantum critical scaling as observed in metallic quantum critical systems,[9] however, next we argue that its response shows all the hallmarks of E/T scaling; hallmarks that were thought to be associated exclusively with quantum criticality. We argue, without using any particular line-shape analysis, that scattering originating from the superspins effectively mimics quantum scaling behavior and that this scaling can be observed even in the compound that displays long-range ordering ($x=0.2$).

Lamsal *et al.*[28] have shown that the data taken in the pilot experiment[38] on the fully lithiated compound ($x=1.0$) display what looks like E/T scaling for $T=30$, 50, and 70 K. We extend these observations to all concentrations x in order to show that the mimicking of E/T-scaling behavior is present for all x, even when long-range order is present at low temperatures ($x=0.2$). To demonstrate this, we plot the full response for $T=24$, 33, 41, and 100 K as a function of E/T for all four concentrations x in Fig. 8. In order to achieve the scaling between the various temperatures in this figure, we have first scaled each q value to the magnetic form factor as was done in Fig. 7 with the caveat that the form factor $M(q)$ is now determined for all temperatures from the scattering at $I(q,E/k_BT=0.17)$. This particular choice anticipates E/T-scaling behavior. That is, the shape of the form factor can be determined from any energy transfer E (see Fig. 6), but in order to be able to directly compare the scattered intensity at various temperatures we must take into account that the scattering moves to lower E with decreasing T. Thus, a cut at $E=0.6$ meV at 41 K to determine $M(q)$ would yield the same q dependence as a cut at $E=0.6$ meV at 25 K, but it would yield a higher value overall for $M(q)$. Instead, taking the cut at $E/k_BT=0.17$ takes the temperature dependence into account in a manner self-consistent with E/T scaling. In addition, we took out the thermal population factors in order

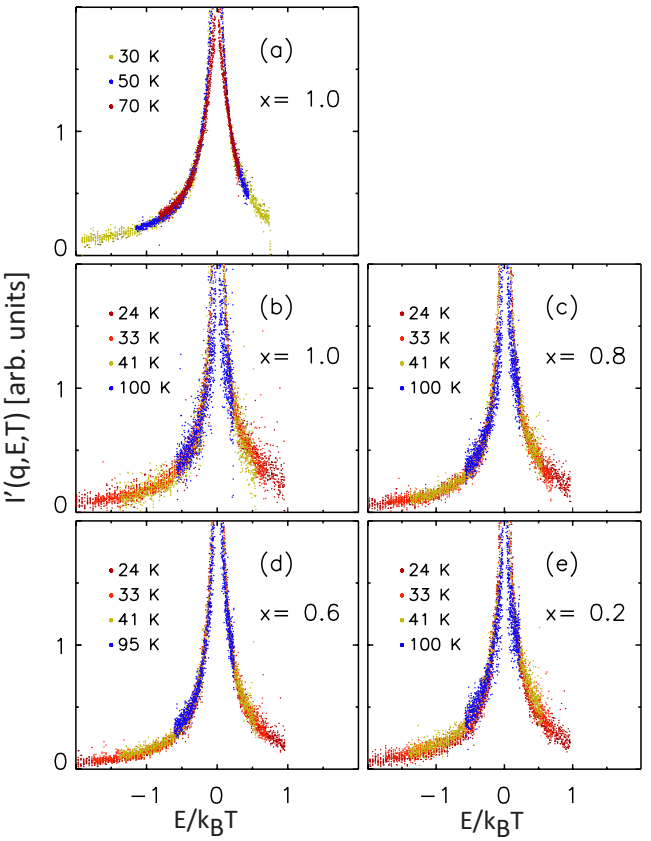

FIG. 8. (Color online) Same as Fig. 7, but now the data have been corrected for (trivial) temperature effects [Eq. (2)] and they have been plotted versus E/k_BT (circles). The data in part (a) are the ILL data of the pilot experiment, Ref. 38, parts (b)–(e) correspond to the new ILL experiments. The Li concentrations x and temperatures are shown in the figure. All curves collapse into one curve, giving the appearance of dynamical scaling. The finite energy resolution (Fig. 3) of the spectrometer causes the apparent differences between the temperatures for $|E/k_BT|<0.1$.

to arrive at the function $I'(q,E,T)$ plotted in Fig. 8

$$I'(q,E,T) = I(q,E,T)\frac{(1-e^{-E/k_BT})}{I(q,E/k_BT=0.17)(E/k_BT)}. \quad (2)$$

The function $I'(q,E,T)$ is, in fact, the Fourier transform of the relaxation function of the spin excitations in the system. As can be seen in Fig. 8, $I'(q,E,T)$ appears to depend on E/T as a single variable rather than on E and T separately. That is, all curves coincide to such an extent that E/T-scaling behavior seems to take place. Even at the lowest temperature ($T=24$ K, close to the temperature where the superspins are starting to freeze out[35,36,38,39]) and at the highest temperature ($T=100$ K, above the temperature where the Mn^{4+} ions in the clusters have fully lined up), the line shape of the response is still remarkably similar to the data taken at $T=33$ and 41 K.

In Fig. 9(a) we show the TRIAX data at $q=1.4$ Å^{-1} for $5<T<70$ K. This is the q value that corresponds to the strongest scattering for the fully lithiated compound (Fig. 5). As can be seen in this figure, the scattering appears to depend only on the ratio of E/T, not on E and T as separate vari-

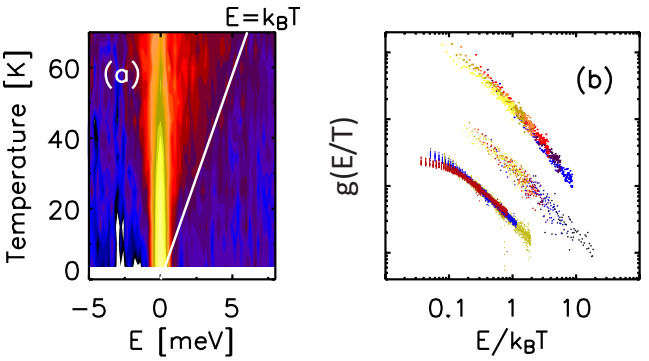

FIG. 9. (Color online) (a) The magnetic scattering of the fully lithiated compound ($x=1.0$) measured at $q=1.4$ Å^{-1} on TRIAX. The intensity scale is the same as for in Fig. 4. The scattering behaves as if E/T is the only relevant variable: the scattering intensity develops along straight lines $E\sim T$ such as the white line $E=k_BT$ shown in the figure. (b) When $g(E/T)$ [Eq. (3)] is plotted on a log-log scale, the scattering appears to display dynamical scaling over the full range. The lower curve are the ILL data from Fig. 8(a), the middle curve are all the TRIAX data shown in part (a) of this figure, and the upper curve are the data for $Ce(Ru_{0.24}Fe_{0.76})_2Ge_2$ at $q=0.4$ Å^{-1} (Ref. 15). The three curves are offset for plotting clarity.

ables. This E/T dependence appears to reach down to the lowest temperatures, and certainly appears to mimic E/T scaling when plotted [see Fig. 9(b)] on a log-log scale as is usually done[12–15] in QCP systems.

Independent of whether we include the data at $T=100$ K and at the very lowest temperatures or not, it is clear that the E/T-scaling mimicking survives for a wide range of cluster morphologies, even into the range of compositions where long-range order coexists with short-range ordered clusters. This implies that the energy barrier Δ that controls the reorientation of the total cluster spin is likely to be small, a result that was to be anticipated based on the findings[27] in $ZnCr_2O_4$. The range of compositions studied in our spinel system corresponds to a similar range of compositions investigated for QCP systems close to the 0 K order-disorder transition where isolated magnetic clusters of various sizes are present[18] [Fig. 1(e)], and would also cover the ordered phase where a lattice spanning cluster [Fig. 1(d)] is present in addition to smaller, isolated ones. Therefore it would appear that in all these cases E/T scaling should be strongly influenced by the emergence of magnetic clusters, independent of the actual underlying quantum critical behavior associated with a competition between ordering and shielding.

Of the quantum critical systems reported in the literature, the magnetic response of our classical system seems to be closest to that found in $UCu_{5-x}Pd_x$.[13,14] For instance, the static structure factor of $UCu_{5-x}Pd_x$ ($x=1$ and 1.5)[13,14] is very similar to that of our spinel compound and its dynamics similarly demonstrates a lack of q dependence when plotted as in Fig. 8, which implies that magnetic clusters could be forming in $UCu_{5-x}Pd_x$ ($x=1$ and 1.5) making it much harder to distinguish between classical physics and quantum critical response. Thus, if we are to distinguish quantum critical scaling from geometry-induced mimicking of scaling, then we must scrutinize the scaling function itself. In the present work we have found a scaling relation that can be cast into a similar form as the scaling functions found in the literature[12–16,40]

$$I'(q,E,T)\sim\frac{\chi''(q,E,T)}{M(q)(E/k_BT)}=g(E/T^b)/T^a. \tag{3}$$

For our classical system we find $a=0$ and $b=1$ for the exponents. Aronson *et al.*[13,14] found that $UCu_{5-x}Pd_x$ scales with $a=1/3$ and $b=1$ in their original observation of scaling in QCP systems. Further, Schröder *et al.*,[12] Knafo *et al.*,[40] and Montfrooij *et al.*[15] each found differing values in the systems $CeCu_{6-x}Au_x$ ($a=0.75$ and $b=1$), $Ce_{0.925}La_{0.075}Ru_2Si_2$ ($a=1$ and $b=0.8$), and $Ce(Ru_{0.24}Fe_{0.76})_2Ge_2$ ($a=0.51$ and $b=1$), respectively. More recently, Krishnamurthy *et al.*[16] reported an exponent of $a=0.2-0.5$ (and $b=1$) for $URu_{2-x}Re_xSi_2$ for $x=0.2-0.6$, respectively. Note that it is not clear at present, given the range of values reported for the exponent a, whether there is an underlying connection between the exponent a of the scaling relation and the ratio d/z of the effective dimension d and the dynamical exponent z.

Whereas the static structure factor of quantum critical $UCu_{5-x}Pd_x$ closely resembles that of our classical spinel system, $Ce(Ru_{0.24}Fe_{0.76})_2Ge_2$ displays a structure factor that is nonlocal with an incommensurate ordering wave vector of $\vec{Q}=(0,0,0.45)$. Yet, when we plot $g(E/T)$ for $Ce(Ru_{0.24}Fe_{0.76})_2Ge_2$ [Fig. 9(b)] we find that the quantum critical scaling of this system closely resembles that of our classical system (at least) near its ordering wave vector $q=0.4$ Å^{-1} (Refs. 15 and 18) and for the range of temperatures $T=1.9$, 2.9, 4.4, 7.5, 10.4, and 15.4 K. Then, for chemically disordered quantum critical systems, it might well be that the observed E/T scaling is largely determined by the presence of magnetic clusters that form because of a distribution in Kondo temperatures. The main difference between classical and quantum critical systems would then be in the actual value of the exponent a.

In conclusion, we have shown that the dynamical response of the magnetic clusters in $Li_x[Mn_{1.96}Li_{0.04}]O_4$ mimics E/T-scaling behavior. Similar magnetic clusters are expected to be present[18] in quantum critical systems that have been driven to the QCP by means of (substantial) chemical doping, and therefore, the E/T scaling observed in these latter systems is expected to be strongly influenced by the emergence of magnetic clusters. Our findings apply both to quantum critical systems that seem to be dominated by local physics ($UCu_{5-x}Pd_x$) as well as to systems that show incommensurate long-range order [$Ce(Ru_{0.24}Fe_{0.76})_2Ge_2$]. We suggest that these systems should no longer be assumed, *a priori*, to behave as a collection of magnetic moments that all undergo shielding at the same temperature.[7] Our results provide a way to reconcile both possible scenarios for a quantum phase transition [as depicted in Figs. 1(a) and 1(b)] with the measured data, by modifying these phase diagrams to include the effects of chemical disorder that locally leads to lattice expansion and contraction [Fig. 1(c)]. Detailed lineshape analysis of the scaling curves in both classical and quantum critical systems [Fig. 9(b)] must now be carried out in order to determine which part of the response should be

attributed to geometric effects and which part to purely quantum-mechanical effects.

We are currently investigating, by way of Monte Carlo simulations, what influence a distribution of Kondo-shielding temperatures—leading to cluster formation—would have on the specific heat of a quantum critical system and whether it would be possible that cluster formation might even take place in QCP systems that are close to stoichiometric compositions, such as $CeCu_{6-x}Au_x$. The latter proposition is pure speculation at this point; it is based on the premise that the zero-point motion of the lattice ions would be sufficient to change interatomic distances by a very small amount, leading to a distribution of Kondo-shielding temperatures that would in turn automatically lead to the formation of clusters. The morphology of these clusters would change as a function of time. Whether this process is actually relevant or not to the physics near the QCP would depend on whether the conduction electrons would move on a faster time scale than the zero-point motion of the ions or not.

ACKNOWLEDGMENTS

This research is supported by the U. S. Department of Energy, Office of Basic Energy Sciences, and the Division of Materials Sciences and Engineering under Grant No. DE-FG02-07ER46381. J. G. is supported by the University of Missouri Research Board (Grant No. RB-07-52). T.V. is supported by the National Science Foundation (Grant No. DMR-0339147) and the Research Corporation. The authors are indebted to Hannu Mutka for invaluable assistance with running the measurements at the Institut Laue-Langevin.

[1] M. B. Maple, D. A. Gajewski, Y. Dalichaouch, V. B. Barbetta, M. C. Andrade, H. A. Mook, H. G. Lukefahr, O. O. Bernal, and D. E. MacLaughlin, J. Low Temp. Phys. **95**, 225 (1994).
[2] S. R. Julian, C. Pfleiderer, F. M. Grosche, N. D. Mathur, G. J. McMullan, A. J. Diver, I. R. Walker, and G. G. Lonzarich, J. Phys.: Condens. Matter **8**, 9675 (1996).
[3] M. A. Ruderman and C. Kittel, Phys. Rev. **96**, 99 (1954).
[4] T. Kasuya, Prog. Theor. Phys. **16**, 45 (1956).
[5] K. Yosida, Phys. Rev. **106**, 893 (1957).
[6] J. H. Van Vleck, Rev. Mod. Phys. **34**, 681 (1962).
[7] S. Doniach, in *Valence Instabilities and Related Narrow Band Phenomena*, edited by R. D. Parks (Plenum, New York, 1977), p. 169.
[8] S. Sachdev, *Quantum Phase Transitions* (Cambridge University Press, Cambridge, England, 1999).
[9] G. R. Stewart, Rev. Mod. Phys. **73**, 797 (2001).
[10] John. A. Hertz, Phys. Rev. B **14**, 1165 (1976).
[11] A. J. Millis, Phys. Rev. B **48**, 7183 (1993).
[12] A. Schröder, G. Aeppli, R. Coldea, M. Adams, O. Stockert, H. v. Löhneysen, E. Bucher, R. Ramazashvili, and P. Coleman, Nature (London) **407**, 351 (2000).
[13] M. C. Aronson, R. Osborn, R. A. Robinson, J. W. Lynn, R. Chau, C. L. Seaman, and M. B. Maple, Phys. Rev. Lett. **75**, 725 (1995).
[14] M. C. Aronson, R. Osborn, R. Chau, M. B. Maple, B. D. Rainford, and A. P. Murani, Phys. Rev. Lett. **87**, 197205 (2001).
[15] W. Montfrooij, M. C. Aronson, B. D. Rainford, J. A. Mydosh, A. P. Murani, P. Haen, and T. Fukuhara, Phys. Rev. Lett. **91**, 087202 (2003).
[16] V. V. Krishnamurthy, D. T. Adroja, N. P. Butch, S. K. Sinha, M. B. Maple, R. Osborn, J. L. Robertson, S. E. Nagler, and M. C. Aronson, Phys. Rev. B **78**, 024413 (2008).
[17] Qimiao Si, Silvio Rebello, Kevin Ingersent, and J. Lleweilun Smith, Nature (London) **413**, 804 (2001).
[18] W. Montfrooij, J. Lamsal, M. Aronson, M. Bennett, A. de Visser, H. Y. Kai, N. T. Huy, M. Yethiraj, M. Lumsden, and Y. Qiu, Phys. Rev. B **76**, 052404 (2007).
[19] A. H. Castro Neto and B. A. Jones, Phys. Rev. B **62**, 14975 (2000).
[20] M. J. Thill and D. A. Huse, Physica A **214**, 321 (1995).
[21] T. Vojta, J. Phys. A **39**, R143 (2006).
[22] E. Miranda, V. Dobrosavljevic, and G. Kotliar, J. Phys.: Condens. Matter **8**, 9871 (1996).
[23] H. Sugawara, Y. Aoki, H. Sato, N. Mushnikov, and T. Goto, J. Phys. Soc. Jpn. **68**, 1094 (1999).
[24] M. B. Fontes, M. A. Continentino, S. L. Bud'ko, M. El-Massalami, L. C. Sampaio, A. P. Guimaraes, E. Baggio-Saitovitch, M. F. Hundley, and A. Lacerda, Phys. Rev. B **53**, 11678 (1996).
[25] Dietrich Stauffer and Amnon Aharony, *Introduction to Percolation Theory* (CRC, Boca Raton, FL, 1994).
[26] W. Montfrooij, M. C. Aronson, B. D. Rainford, J. A. Mydosh, R. Hendrikx, T. Gortenmulder, A. P. Murani, P. Haen, I. Swainson, and A. de Visser, Phys. Rev. B. **73**, 140401(R) (2006).
[27] S.-H. Lee, C. Broholm, W. Ratcliff, G. Gasparovic, Q. Huang, T. H. Kim, and S.-W. Cheong, Nature (London) **418**, 856 (2002).
[28] J. Lamsal, J. Gaddy, M. Petrovic, W. Montfrooij, and T. Vojta, J. Appl. Phys. **105**, 07E322 (2009).
[29] J. Gaddy, J. Lamsal, M. Petrovic, W. Montfrooij, A. Schmets, and T. Vojta, J. Appl. Phys. **105**, 07D532 (2009).
[30] M. M. Thackeray, J. Am. Ceram. Soc. **82**, 3347 (1999).
[31] J. Rodriguez-Carvajal, G. Rousse, C. Masquelier, and M. Hervieu, Phys. Rev. Lett. **81**, 4660 (1998).
[32] J. E. Greedan, C. R. Wiebe, A. S. Wills, and J. R. Stewart, Phys. Rev. B **65**, 184424 (2002).
[33] I. Tomeno, Y. Kasuya, and Y. Tsunoda, Phys. Rev. B **64**, 094422 (2001).
[34] V. W. J. Verhoeven, F. M. Mulder, and I. M. de Schepper, Physica B **276-278**, 950 (2000).
[35] C. T. Kaiser, V. W. J. Verhoeven, P. C. M. Gubbens, F. M. Mulder, I. de Schepper, A. Yaouanc, P. Dalmas de Reotier, S. P. Cottrell, E. M. Kelder, and J. Schoonman, Phys. Rev. B **62**, R9236 (2000).
[36] J. Sugiyama, K. Mukai, Y. Ikedo, P. L. Russo, T. Suzuki, I. Watanabe, J. H. Brewer, E. J. Ansaldo, K. H. Chow, K. Ariyoshi, and T. Ohzuku, Phys. Rev. B **75**, 174424 (2007).
[37] J. E. Greedan, N. P. Raju, A. S. Wills, C. Morin, and S. M. Shaw, Chem. Mater. **10**, 3058 (1998).

[38] H. G. Schimmel, W. Montfrooij, G. J. Kearley, V. W. J. Verhoeven, and I. M. de Schepper, Phys. Rev. B **63**, 214409 (2001).
[39] T. Heitmann, J. Gaddy, J. Lamsal, M. Petrovic, and W. Montfrooij (unpublished).
[40] W. Knafo, S. Raymond, J. Flouquet, B. Fåk, M. A. Adams, P. Haen, F. Lapierre, S. Yates, and P. Lejay, Phys. Rev. B **70**, 174401 (2004).